

IMPACT OF CASTING SPEED ON THE TEMPERATURE FIELD OF CONTINUOUSLY CAST STEEL BILLETS

VPLIV LIVNE HITROSTI NA TEMPERATURNO POLJE KONTINUIRNO ULITIH GREDEC IZ JEKLA

Lubomir Klimes¹, Josef Stetina¹, Pavol Bucek²

¹Brno University of Technology, Faculty of Mechanical Engineering, Technická 2896/2, 616 69 Brno, Czech Republic

²Zelezniarne Podbrezova, Research and Development Center, Kolkaren 35, 976 81 Podbrezova, Slovakia
klimes@fme.vutbr.cz

Prejem rokopisa – received: 2012-08-31; sprejem za objavo – accepted for publication: 2013-01-04

In continuous casting, the casting speed is one of the most important parameters that influence the entire process of steel production and its productivity. From the physical point of view, the casting speed affects the temperature field formation along the cast steel blank, e.g., the surface and corner temperatures as well as the solidification of the steel, e.g., the shell thickness, the isosolidus and isoliquidus curves, the metallurgical length and the width of the mushy zone. In order to achieve a particular steel structure, the temperature ranges in particular positions (e.g., due to the straightening), and to minimize the occurrence of defects, it is very important to pay attention to a proper determination of the casting speed. The aim of this paper is to investigate the impact of the casting speed on the temperature field formation of continuously cast steel billets, and on the aforementioned parameters. Three steel grades with various chemical compositions and the originally implemented numerical model of the transient temperature field of continuously cast billets in Zelezniarne Podbrezova in Slovakia were utilized for the analysis. The results proved the significant influence of the casting speed on the temperature field formation and on related parameters. The conclusions may be utilized, e.g., for the determination of the casting speed and for the setup of the caster.

Keywords: continuous casting, casting speed, dynamic solidification model, temperature field

Pri kontinuirnem ulivanju je hitrost ulivanja eden od odločilnih parametrov, ki vplivajo na celoten proces proizvodnje jekla in na storilnost. Iz fizikalnega vidika hitrost ulivanja vpliva na nastanek temperaturnega polja vzdolž jeklene gredice, kot na primer na temperaturo robov in površine ulitega bloka, kot tudi na strjevanje jekla, kot na primer debelina strjene skorje, krivulje izosolidusa in izoliquidusa, metalurška dolžina in širina kašastega področja. Da bi dosegli želeno strukturo jekla, temperaturno področje v določenih položajih (npr. zaradi ravnanja) in da bi zmanjšali nastanek poškodb, je zelo pomembno, da smo pozorni na pravilno določitev hitrosti ulivanja. Namen prispevka je raziskati vpliv hitrosti ulivanja na oblikovanje temperaturnega polja pri kontinuirno ulitih gredicah in na že navedene parametre. Za analize so bila uporabljena tri različna jekla z različnimi kemijskimi sestavami in originalen numerični model prehodnega temperaturnega polja gredic v Zelezarni Podbrezova na Slovaškem. Rezultati potrjujejo pomemben vpliv hitrosti ulivanja na nastanek temperaturnega polja in s tem povezanih parametrov. Ugotovitve se lahko uporabijo na primer za določitev hitrosti ulivanja in za postavitev livne naprave.

Ključne besede: kontinuirno ulivanje, hitrost ulivanja, dinamični model strjevanja, temperaturno polje

1 INTRODUCTION

The quality and productivity of continuously cast steel blanks depend on many technological parameters and caster options.¹ The casting speed, which is directly related to the productivity, is one of the most important parameters for continuous steel casting. Its appropriate setting according to the operating conditions, the steel grade being cast and the caster parameters is crucial in order to produce steel blanks with the desired quality and structure, and also to minimize the occurrence of defects. In addition, the produced steel and its properties can be further optimized.² The importance of the proper setting of the casting speed is obvious when taking into account the parameters on which the casting speed may have an influence: mainly the entire temperature distribution (e.g., the surface and corner temperatures that are very often required to fit a certain range of temperatures, e.g., due to the straightening) along the cast blank, the isosolidus and isoliquidus curves that characterize the solidification process, the metallurgical length, or, e.g., the shell thickness along the blank.³

Nowadays, dynamic solidification models are commonly used in steelworks for the control and monitoring of casting.^{4,5} The on-line models for the casting control are fast and rather simple, whereas the off-line models enable an analysis of multiple and detailed factors, but require a long time to run.⁶ Numerical models of the temperature field of continuous casting often utilize the finite-difference method,⁷ the finite-volume method⁸, or the finite-element method.⁹ Recently, new computational approaches are also used, due to their specific advantages, e.g., the meshless finite-point method,¹⁰ the front-tracking boundary-element method,¹¹ or the very fast moving-slice-based models.¹²

The numerical solidification models allow a precise determination of the entire temperature distribution along the cast blank, the prediction of surface defects and the improvement of steel quality.¹³ The numerical model in the off-line mode working as a simulator also makes it possible to perform a case study and an analysis of the operating parameters without any affect on the real caster and the steel production in a steelworks.⁶ Hence, it

is a good idea to utilize the dynamic solidification models in order to determine a suitable casting speed for continuously cast blanks.

The purpose of this paper is to investigate the influence of the casting speed on the temperature field formation and the related parameters of continuously cast billets. For the analysis, three steel grades and the 200 mm × 200 mm billets, which are cast in Zeleziarne Podbrezova in Slovakia, are considered. The analysis was carried out by means of the originally implemented dynamic solidification model of continuously cast billets.

2 DYNAMIC SOLIDIFICATION MODEL

The study of the influence of the casting speed on the thermal behavior of continuously cast steel billets was performed with the use of the originally developed numerical model of the transient temperature field.^{14,15} The model, which is fully 3D, allows a calculation of the transient temperature distribution along the entire, continuously cast billets from the pouring level inside the mould, through the secondary and tertiary cooling zones, to the torch where the semi-infinite billets are cut to desired lengths suitable for the next processing step (**Figure 1**). Since the temperature field is symmetric with respect to the longitudinal vertical plane (**Figure 1**), only one half of the billet is considered.

The transient heat transfer and the solidification of the billet is governed by the Fourier-Kirchhoff equation:

$$\frac{\partial H}{\partial t} = \nabla \cdot (k \nabla T) + v_z \frac{\partial H}{\partial z} \quad (1)$$

where H is the volume enthalpy (J m^{-3}), T is the temperature (K), t is time (s), k is the thermal conductivity ($\text{W m}^{-1} \text{K}^{-1}$), v_z is the casting speed (m s^{-1}) and z is the spatial coordinate along the cast billet (m). The mass transfer and the fluid flow of the melt inside the billet are neglected. The thermodynamic function of the volume enthalpy¹⁶ in Eq. (1), which is defined as follows:

$$H(T) = \int_0^T \left(\rho c - \rho L_f \frac{\partial f_s}{\partial \theta} \right) d\theta \quad (2)$$

where ρ is the density (kg m^{-3}), c is the specific heat ($\text{J kg}^{-1} \text{K}^{-1}$), L_f is the latent heat (J kg^{-1}) and f_s is the solid fraction (1), is used due to the release of the latent heat of structural and mainly phase changes, which the steel undergoes during its solidification.¹⁷

The model is completed with the initial (3) and boundary conditions (4a)–(4d):

$$T_{i,j,k}^0 = T_0 \quad (3)$$

$$T_{i,j,0}^t = T_{\text{cast}} \text{ in the meniscus plane} \quad (4a)$$

$$-k \frac{\partial T}{\partial n} = 0 \text{ in the plane of symmetry} \quad (4b)$$

$$-k \frac{\partial T}{\partial n} = \dot{q} \text{ in the mould and beneath the rollers} \quad (4c)$$

$$-k \frac{\partial T}{\partial n} = h(T - T_\infty) + \sigma \varepsilon (T^4 - T_\infty^4) \text{ in the secondary and tertiary cooling zones} \quad (4d)$$

where T_0 is the initial temperature (K), T_{cast} is the casting temperature (K), \dot{q} is the heat flux (W m^{-2}), h is the heat transfer coefficient ($\text{W m}^{-2} \text{K}^{-1}$), T_∞ is the ambient temperature (K), $\sigma = 5.67 \cdot 10^{-8} \text{ W m}^{-2} \text{K}^{-4}$ is the Stefan-Boltzmann constant and ε is the emissivity (1).

In order to accurately and reliably predict the temperature field of cast blanks by means of solidification models, it is also worth pointing out the variability of the thermophysical properties (H , k , ρ , c : see Eq. (1) and Eq. (2)) according to the chemical composition of the steel being cast and their dependency on the temperature. Due to the mentioned reasons, the developed solidification model utilizes the results of the solidification analysis package IDS.¹⁸ It enables the calculation of the temperature dependency of the aforementioned thermophysical properties according to the chemical composition of the steel. The precise chemical composition can be obtained, e.g., from the chemical analysis of a sample from the tundish.

The dynamic solidification model of continuously cast billets was created with the use of the control-volume method.¹⁹ This approach is based on meshing the entire 3D billet into control volumes, and then the energy balance is established for each control volume of the billet. With the use of the explicit discretization in time,¹⁹ the energy balance of the general control volume (i, j, k) (**Figures 1** and **2**) in the Cartesian coordinates reads:

$$\sum_{i=1}^6 \dot{Q}_i + v_z \Delta x \Delta y (H_{i,j,k-1}^t - H_{i,j,k}^t) = \frac{\Delta x \Delta y \Delta z}{\Delta t} (H_{i,j,k}^{t+\Delta t} - H_{i,j,k}^t) \quad (5)$$

where \dot{Q} denotes the heat transfer rate (W), Δx , Δy , Δz are the spatial dimensions (m) of the control volume and

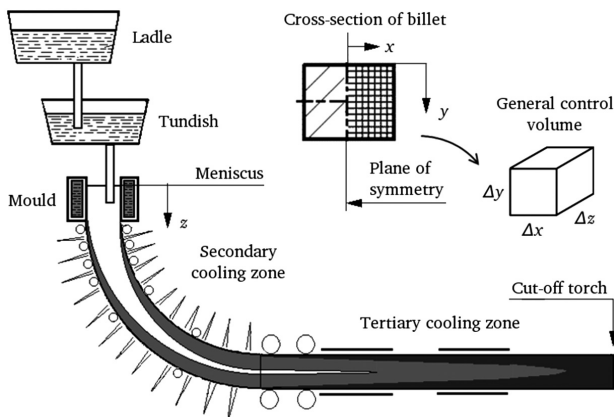


Figure 1: The billet caster and the mesh definition
Slika 1: Naprava za ulivanje gredic in opredelitev mreže

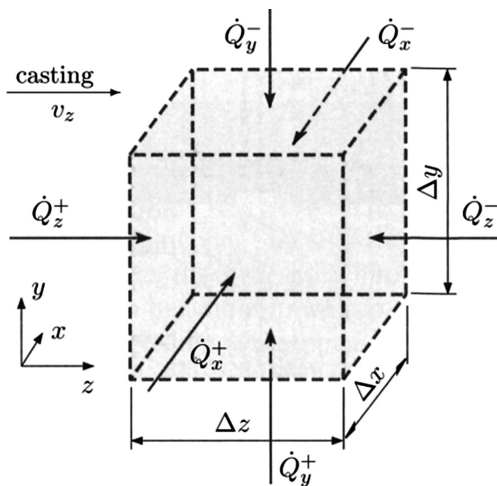


Figure 2: The energy balance of the general control volume in Cartesian coordinates

Slika 2: Energijska bilanca splošnega kontrolnega volumna v kartezičnih koordinatah

Δt is the time step (s). The first term on the left-hand side in Eq. (5) represents the sum of the conduction heat transfer rates given by Fourier's law¹⁹ to the control volume from the neighboring six control volumes (**Figure 2**). For instance, the heat transfer rate to the control volume in the positive direction of the x -axis is then:

$$\dot{Q}_x^+ = -k\Delta y\Delta z \frac{T_{i,j,k}^t - T_{i-1,j,k}^t}{\Delta x} \quad (6)$$

The second term on the left-hand side in Eq. (5) takes into account the energy incoming to the control volume due to the movement of the billet through the caster with the casting speed v_z . The term on the right-hand side in Eq. (5) represents the change of the internal energy of the control volume during the time step Δt , including the release of the latent heat (comprised in the enthalpy) due to the solidification.^{16,17}

In the case of the explicit time discretization,¹⁹ the unknown enthalpy of the general control volume (i, j, k) in time $t + \Delta t$ can be then directly calculated from Eq. (5) with the use of known values of the temperature and enthalpy in time t :

$$H_{i,j,k}^{t+\Delta t} = H_{i,j,k}^t + \frac{\Delta t}{\Delta x\Delta y\Delta z} \sum_{i=1}^6 \dot{Q}_i + v_z \frac{\Delta t}{\Delta z} (H_{i,j,k-1}^t - H_{i,j,k}^t) \quad (7)$$

In the case of the boundary-control volume, the particular heat transfer rates in Eq. (7) are replaced by the corresponding heat transfer rates determined from the boundary conditions (4a)–(4d). The desired temperature in time $t + \Delta t$ is then recalculated from the enthalpy given by Eq. (7) with the use of the temperature-enthalpy relationship provided by the solidification package IDS according to the particular chemical composition of the cast steel.

In the curved region (the radial part) of the caster, the Cartesian coordinate system is transformed to the cylindrical system (the Cartesian coordinates y and z are transformed to the radius coordinate and to the angle coordinate, respectively) and the equations (5)–(7) are appropriately modified.

The model used in the presented analysis utilizes 1136520 control volumes (21 in axis x , 41 in axis y , and 1320 in axis z) with the size of the general control volume of 5 mm \times 5 mm \times 15 mm. Due to the unconditional stability¹⁹ of the explicit time discretization and the numerical stability also for higher casting speeds, the time step was set to 0.35 s. With the described configuration of the mesh and the time step, the numerical model is still able to run faster than real time. For example, on the HP Z800 workstation the computing time reaches 90 % of the real time.²⁰

The heat transfer coefficients in the boundary condition (4d) for the cooling nozzles in the secondary cooling were determined experimentally in the laboratory on the hot models.²¹ **Figure 3** presents the experimentally measured heat-transfer coefficient for the cooling nozzle TG1 used in the secondary cooling. In order to quantify the heat withdrawal in the mould and the secondary cooling zone,²⁰ the heat flux in the mould given by Eq. (4c) was equivalently expressed to the heat transfer coefficient and plotted in **Figure 4**.

As can be seen from Eq. (1), Eq. (5), and Eq. (7), the casting speed v_z straightforwardly influences the entire transient temperature distribution of cast billets, and therefore the appropriate setting of the casting speed is a crucial issue in continuous casting.

The developed dynamic solidification model was experimentally verified on the billet caster with the use

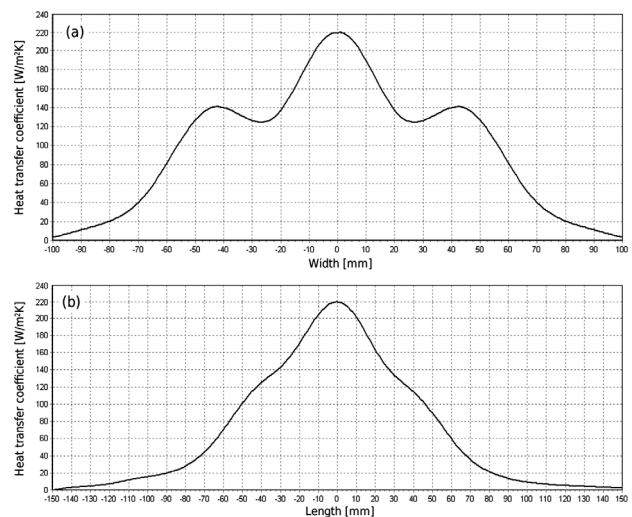


Figure 3: The heat transfer coefficient for the cooling nozzle TG1 and the water flow 0.64 l/min in the centerline of the nozzle: a) perpendicular to the casting direction, b) along the casting direction

Slika 3: Koeficient prenosa toplote za hladilno šobo TG1 in pretok vode 0,64 l/min v simetrali šob: a) pravokotno na smer ulivanja, b) vzdolž smeri ulivanja

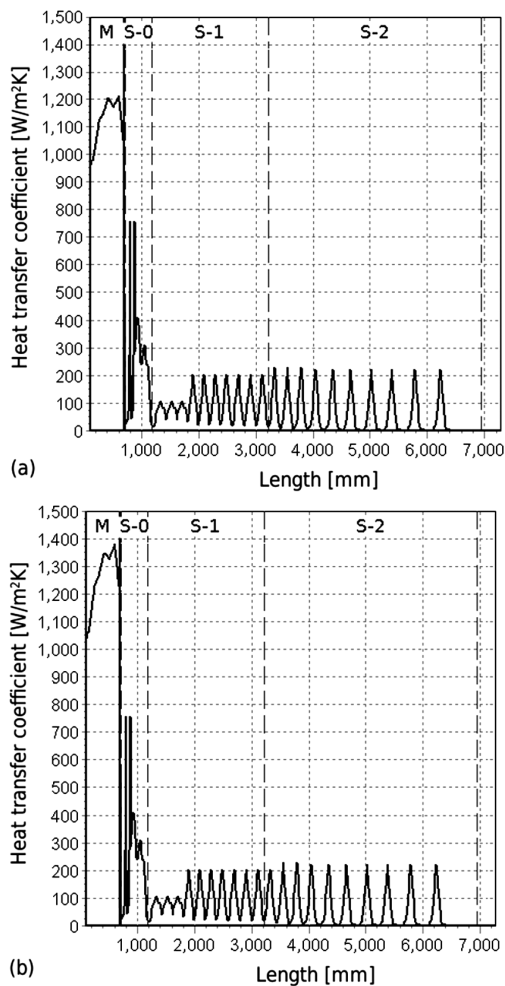


Figure 4: The heat transfer coefficient in the mould and in the secondary cooling zone: a) small radius surface, b) large radius surface of cast billet

Slika 4: Koeficient prenosa toplote v kokili in v sekundarni coni hlajenja: a) površina z majhno ukrivljenostjo, b) površina z veliko ukrivljenostjo lite gredice

of two pyrometers placed behind the mould in the secondary cooling zone (1500 mm from the pour level) and in the tertiary cooling zone (15420 mm from the pour level). Both the pyrometers were positioned in the centerline of the small radius surface of the cast billets. The maximum temperature difference between the measured temperatures by the pyrometers and the calculated temperatures by the solidification model was 40 °C.²⁰

3 ANALYSIS SETUP AND PARAMETERS

The study was carried out for the 200 mm × 200 mm steel billets that are continuously cast in Zeleziarne Podbrezova in Slovakia. The radial billet caster has the tubal mould, it comprises the secondary cooling with three independent cooling zones (denoted by S-0, S-1, and S-2 in figures) including 96 water cooling nozzles of three

types and two straightening mills (denoted by SM-1, SM-2 in figures).

The following three steel grades are considered (only the main elements are listed in mass fractions *w*): unalloyed fine-grained steel for constructions and welding S355J2G3 (0.187 % C, 1.17 % Mn, 0.22 % Si, 0.016 % P, and 0.012 % S), carbon steel for refining C60 (0.617 % C, 0.73 % Mn, 0.29 % Si, 0.014 % P, 0.013 % S, 0.03 % Cr, 0.05 % Ni, and 0.18 % Cu), and heat-resistant Cr-Mo steel for use at higher temperatures 13CrMo4-5 (0.144 % C, 0.53 % Mn, 0.24 % Si, 0.007 % P, 0.006 % S, 0.98 % Cr, 0.46 % Mo, 0.12 % Cu, and 0.019 % Al). The range of the casting speed was considered to be between 0.7 m/min and 1.1 m/min; all three mentioned steel grades are commonly cast with a casting speed of 0.9-1.0 m/min. In figures, only the casting speeds 0.7 m/min, 0.9 m/min, and 1.1 m/min are pictured for reasons of clarity.

For the analysis the casting temperature was set identically to the real casting process: 1553 °C for the grade S355J2G3, 1515 °C for the grade C60, and 1547 °C for the grade 13CrMo4-5. The analysis was carried out for the identical setting of the caster, mainly the water flow rates through the cooling nozzles in the secondary cooling and through the mould for all the considered steel grades.

4 RESULTS AND DISCUSSION

4.1 Surface and corner temperatures

The analysis confirmed a significant dependency of the temperature field of the cast billets on the casting speed. For all steel grades, a very similar thermal behavior was observed (**Figure 5** for the steel grade S355J2G3): the higher casting speed, the higher both the corner temperature and the surface temperature beneath the nozzles. Moreover, with an increasing casting speed the rise of both the surface and corner temperatures decreases (**Figure 5**). As already mentioned, although all three investigated steel grades have various chemical

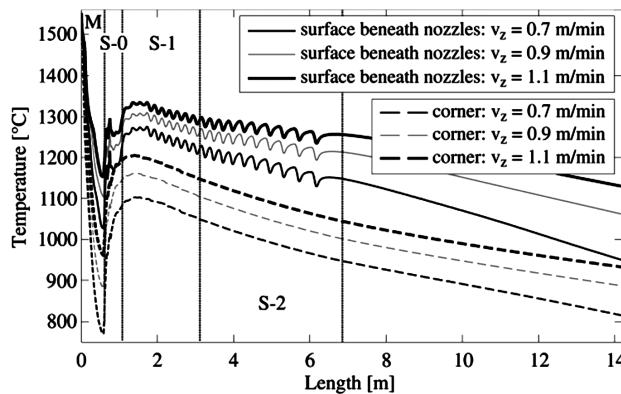


Figure 5: The impact of the casting speed on the surface and corner temperatures for the steel grade S355J2G3

Slika 5: Vpliv hitrosti ulivanja na temperaturo površine in robov pri jeklu S355J2G3

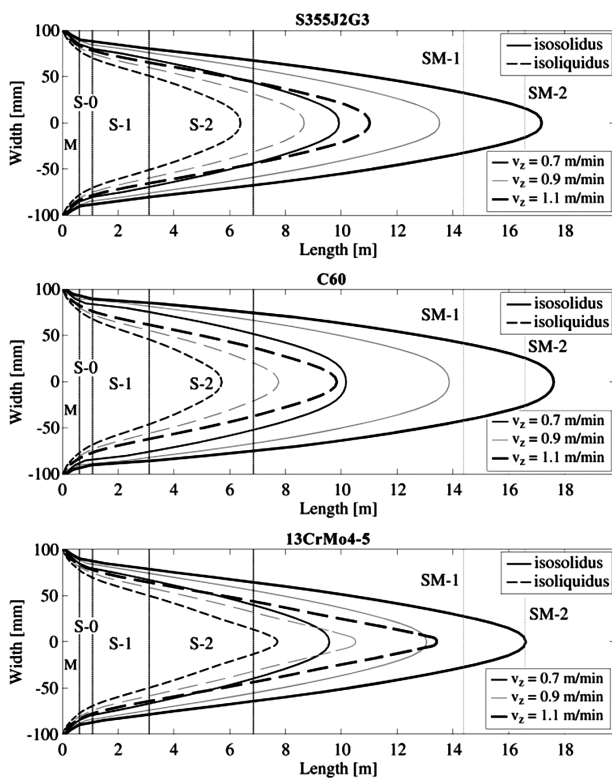


Figure 6: The influence of the casting speed on the isosolidus and isoliquidus curves, and the mushy zone

Slika 6: Vpliv hitrosti ulivanja na izosolidusne, izoliquidusne krivulje in na kašasto področje

compositions and each of them is intended for a different usage, their relative courses of the surface and the corner temperatures along the caster with a casting speed in the range between 0.7 m/min and 1.1 m/min are almost identical. The only significant difference is the temperature shift of both the surface and the corner temperature curves due to the various casting temperatures.

4.2 Isosolidus and isoliquidus curves, metallurgical length, mushy zone

The thermal behavior inside the cast billets, the solidification process, and the influence of the casting

speed on them can be investigated in the longitudinal axial cross-section of the billet with the use of the isosolidus and isoliquidus curves. Moreover, the isosolidus curve is directly related to the metallurgical length, which is an important parameter of continuous casting.

Figure 6 shows the influence of the casting speed on the solidification process of steel in the core of the billets: the isosolidus and isoliquidus curves, and the mushy zone where both the liquid and solid phases coexist.

As can be observed from **Figure 6**, the profile of the isosolidus and isoliquidus curves, the metallurgical length as well as the width of the mushy zone differs for each of the three investigated steel grades. In general, the higher casting speed makes both the isosolidus and isoliquidus longer (a positive shift in the length) and lengthens the metallurgical length as well (**Figure 6**). Moreover, the higher casting speed also enlarges the mushy zone. It implies that the positive shift of the isosolidus curve due to the increasing casting speed is larger than the shift of the isoliquidus curve.

For instance, consider the steel grade C60 (see the middle graph in **Figure 6**): for the casting speed of 0.7 m/min the metallurgical length is 10.1 m and the width of the mushy zone (in the axis of the billet) is 4.5 m. For the casting speed of 0.9 m/min, the metallurgical length increases to 13.9 m and the width of the mushy zone to 6.1 m. However, in the case of the casting speed of 1.1 m/min, the metallurgical length reaches 17.6 m (e.g., in the positions of both the straightening mills SM-1 and SM-2 the billet still contains the liquid phase) and the mushy zones distends to 7.7 m.

4.3 Shell thickness

The casting speed also has an impact on the rate of the shell thickness growth along the caster. A similar shell thickness behavior was observed for all three investigated steel grades. In general, the higher casting speed, the slower rate of the shell thickness growth (**Figure 7**). The shell inside the mould grows almost linearly, and behind the mould the rate of the shell thickness growth declines due to the abrupt reduction of the heat withdrawal. In the secondary cooling the rate of the shell thickness growth slowly increases owing to the

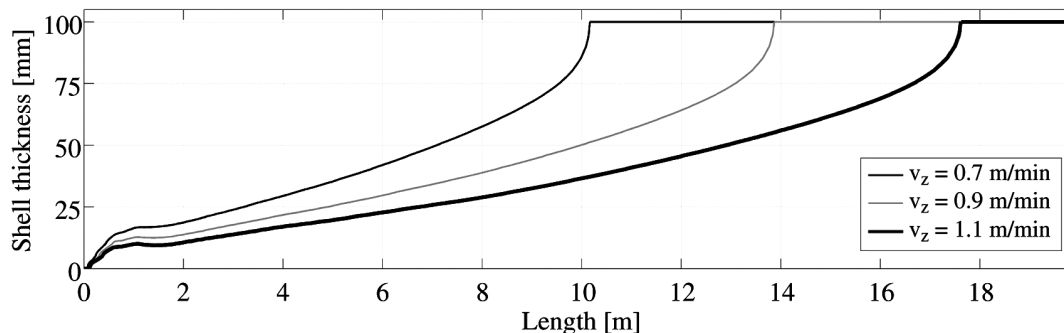


Figure 7: The influence of the casting speed on the shell thickness for the steel grade C60

Slika 7: Vpliv hitrosti ulivanja na debelino skorje pri jeklu C60

heat withdrawal of the cooling nozzles and also of the free convection and radiation heat transfer mechanisms.

For instance, **Figure 7** for the steel grade C60. In the length of 10.1 m where the billet cast with the casting speed of 0.7 m/min is completely solidified (i.e., the shell thickness is 100 mm), the shell thickness of the billet cast with the casting speed of 0.9 m/min is only 50 mm and the shell thickness of the billet cast with the casting speed of 1.1 m/min is even only 35 mm. The billet cast with the casting speed of 0.9 m/min is completely solidified in the length of 13.8 m, where the shell thickness of the billet cast with the casting speed of 1.1 m/min is only 55 mm.

4.4 Local period of solidification

The solidification process of the steel billets can also be investigated by the local period of solidification, which represents the local width of the mushy zone expressed in time related to the casting speed. Thus, for the given point (x, y) in the cross-section of the billet (**Figure 1**), the local period of solidification $lps(x, y)$ expresses the time (s) needed for the solidification (**Figure 6**), i.e., for cooling down from the liquidus temperature (where the first grains of solid phase appear) to the solidus temperature (where the last melt is solidified) along the billet assuming its movement through the caster with the casting velocity:

$$lps(x, y) = \frac{L_{solidus}(x, y) - L_{liquidus}(x, y)}{v_z} \quad (8)$$

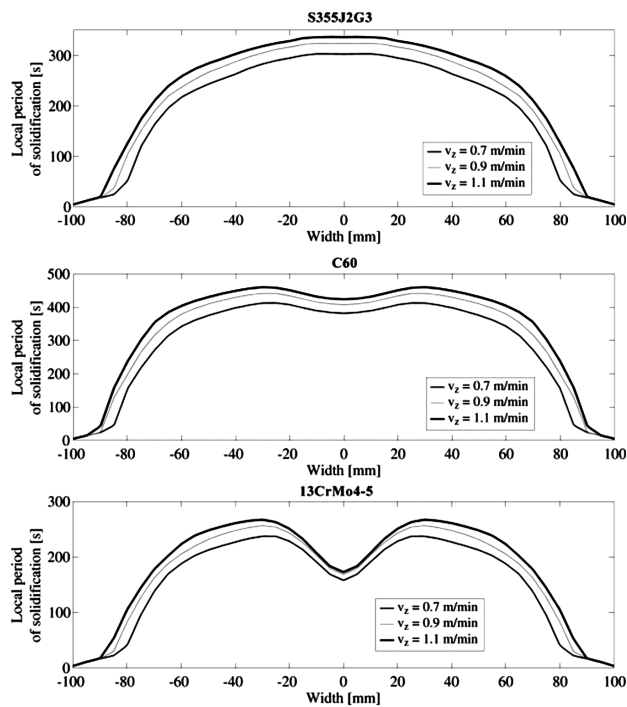


Figure 8: The influence of the casting speed on the local period of solidification in the axial cross-section

Slika 8: Vpliv hitrosti ulivanja na lokalni čas strjevanja v osnem prerezu

where $L_{solidus}(x, y)$ (m) and $L_{liquidus}(x, y)$ (m) are the lengths of the isosolidus and isoliquidus curves in the cross-section point (x, y) (**Figure 6** plotted for $y = 100$ mm), and v_z is the casting velocity ($m\ s^{-1}$). The local periods of solidification in the horizontal centerline of the cross section (i.e., for the cross section points (x, y) for which $y = 100$ mm) of cast billets are shown in **Figure 8**.

In general, a higher casting speed makes the local period of solidification longer (**Figure 8**). However, the profiles of the local periods of solidification are different for particular steel grades. This behavior is mainly caused by the different steel structure attained during the solidification of the particular steel grade directly related to the chemical composition and by the setup of cooling.²⁰ It was shown that a modification of the chemical composition in the range of the chemical composition given by norms and standards can change the profile of the local period of solidification.²²

In the case of the grade S355J2G3, the slowest solidification is in the core of the billet. However, the slowest solidification of the grade C60 is not in the core, but about 30 mm out of the core (width = ± 30 mm in **Figure 8**). The described behavior is even more evident in the case of the grade 13CrMo4-5, where the slowest solidification is in approximately the same position (width = ± 30 mm) as in the case of C60, but it needs an extra 80 s to be solidified than the core of the billet (width = 0 mm).

5 CONCLUSION

The paper presents the results of an analysis aimed at the impact of the casting speed on the temperature field of continuously cast steel billets and related parameters. The analysis was carried out with the use of the originally implemented dynamic solidification and three various steel grades were taken into account: common unalloyed steel for constructions, carbon steel for refining, and anticorrosive Cr-Mo steel for use at higher temperatures. The casting speed in the range between 0.7 m/min and 1.1 m/min was considered.

The performed analysis proved that the casting speed can significantly influence the temperature field and the solidification during the continuous steel casting. In general, the higher casting speed increases the temperature of the cast billets due to a reduced heat withdrawal. Consequently, the isosolidus and isoliquidus curves become longer and it also causes an increase of the metallurgical length. The higher casting speed also causes a drop in the shell growth as well as making the mushy zone wider, which implies a longer local period of solidification.

The study confirmed that the dynamic solidification models make it possible to perform an analysis of the caster and billets responses to various operating conditions and situations. The results can then be used by operators to set-up the caster.

Acknowledgement

The presented research was supported by the project GACR P107/11/1566 of the Czech Science Foundation and by the BUT project FSI-J-12-22. The main author, the holder of Brno PhD Talent Financial Aid sponsored by Brno City Municipality, also gratefully acknowledges that financial support.

6 REFERENCES

- ¹ A. Cramb Ed., Making, shaping and treating of steel: casting, 11th edition, Assn of Iron & Steel Engineers, 2003
- ² P. Popela, Optimizing mechanical properties of iron during melting process, *ZAAM: Zeitschrift für Angewandte Mathematik und Mechanik*, 77 (1997) 2, S649–S650
- ³ M. Sadat, A. H. Gheysari, S. Sadat, The effects of casting speed on steel continuous casting process, *Heat and Mass Transfer*, 47 (2011) 12, 1601–1609
- ⁴ Y. Meng, B. G. Thomas, Heat-Transfer and Solidification Model of Continuous Slab Casting: CON1D, *Metallurgical and materials transactions B*, 34 (2003) 5, 685–705
- ⁵ J. Stetina, L. Klimes, T. Mauder, F. Kavicka, Final-structure prediction of continuously cast billets, *Mater. Tehnol.*, 46 (2012) 2, 155–160
- ⁶ B. G. Thomas, Modeling of the continuous casting of steel-past, present, and future, *Metallurgical and materials transactions B*, 33 (2002) 6, 795–812
- ⁷ B. Petrus, K. Zheng, X. Zhou, B. G. Thomas, J. Bentsman, Real-time, model-based spray-cooling control system for steel continuous casting, *Metallurgical and materials transactions B*, 42 (2011) 1, 87–103
- ⁸ J. C. Ma, Z. Xie, Y. Ci, G. L. Jia, Simulation and application of dynamic heat transfer model for improvement of continuous casting process, *Materials science and technology*, 25 (2009) 5, 636–639
- ⁹ M. Gonzalez, M. B. Goldschmit, A. P. Assanelli, E. F. Berdaguer, E. N. Dvorkin, Modeling of the solidification process in a continuous casting installation for steel slabs, *Metallurgical and materials transactions B*, 34 (2003) 4, 455–473
- ¹⁰ L. Zhang, Y. M. Rong, H. F. Shen, T. Y. Huang, Solidification modeling in continuous casting by finite point method, *Journal of materials processing technology*, 192–193 (2007), 511–517
- ¹¹ A. Fic, A. J. Nowak, R. Bialecki, Heat transfer analysis of the continuous casting process by the front tracking BEM, *Engineering analysis with boundary elements*, 24 (2000) 3, 215–223
- ¹² B. Sarler, R. Vertnik, A. Z. Lorbiecka, I. Vusanovic, B. Sencic, A multiscale slice model for continuous casting of steel, *International conference on modeling of casting, welding and advanced solidification processes*, IOP Conference series – Materials science and engineering, 33 (2012), 012021
- ¹³ C. A. Santos, J. A. Spim, A. Garcia, Mathematical modeling and optimization strategies (genetic algorithm and knowledge base) applied to the continuous casting of steel, *Engineering applications of artificial intelligence*, 16 (2003) 5–6, 511–527
- ¹⁴ J. Stetina, F. Kavicka, T. Mauder, L. Klimes, Transient simulation temperature field for continuous casting steel billet and slab, *Proceedings of METEC InSteelCon 2011*, 13–23
- ¹⁵ J. Stetina, F. Kavicka, The influence of the chemical composition of steels on the numerical simulation of a continuously cast slab, *Mater. Tehnol.*, 45 (2011) 4, 363–368
- ¹⁶ C. R. Swaminathan, V. R. Voller, A general enthalpy method for modeling solidification processes, *Metallurgical transactions B*, 23 (1992) 5, 651–664
- ¹⁷ D. M. Stefanescu, *Science and Engineering of Casting Solidification*, Second edition, Springer, 2009
- ¹⁸ J. Miettinen, S. Louhenkilpi, H. Kytönen, J. Laine, IDS: Thermodynamic-kinetic-empirical tool for modelling of solidification, microstructure and material properties, *Mathematics and computers in simulation*, 80 (2010) 7, 1536–1150
- ¹⁹ F. P. Incropera, D. P. DeWitt, T. L. Bergman, A. S. Lavine, *Principles of heat and mass transfer*, Seventh edition, Wiley, 2012
- ²⁰ J. Stetina, L. Klimes, Analysis of continuous casting of steel billets with the use of the transient 3D numerical model of temperature field, *Technical report for Zeleziarne Podbrezova*, Slovakia, Brno University of Technology, 2011
- ²¹ M. Raudensky, J. Horsky, Secondary cooling in continuous casting and Leidenfrost temperature effects, *Ironmaking and steelmaking*, 32 (2005) 2, 159–164
- ²² L. Klimes, J. Stetina, L. Parilak, P. Bucek, Influence of Chemical Composition of Cast Steel on the Temperature Field of Continuously Cast Billets, *Proceedings of Metal 2012*, Ostrava: Tanger, 2012, 34–39